

THE IMPACT OF EM FIELD ON COMBUSTION

J. Valdmanis, I. Barmina, M. Zaķe, R. Valdmanis, A. Cipijs

Institute of Physics, University of Latvia, 32 Miera str., Salaspils, LV-2169, Latvia

e-Mail: mzfi@sal.lv

The effects of DC and AC electric field at 50 Hz and 13.56 MHz and 41 MHz frequencies on the combustion characteristics of biomass pellets have been investigated using an experimental setup of average power 20–40 kW with continuous pellet feed into the setup at average rates 1.5–3 g/s by applying AC voltage to the flame base, where thermal decomposition of biomass pellets produces the axial flow of volatiles (CO, H₂) determining the formation of the flame reaction zone. The AC and DC electric field effects on the flame composition and combustion efficiency are studied with account of field effects on thermal decomposition of biomass, ignition and combustion of volatiles. Main aspects of EM electric field-induced variations of the combustion characteristics and the formation of field-induced combustion instability are discussed and analyzed.

Introduction. The study of DC and AC electric field effects on the combustion characteristics at thermo-chemical conversion of renewable fuels (different biomass types) still remains important due to the possibility of effective electric field-enhanced thermal decomposition of biomass and ignition of volatiles, determining the variations of the flame shape and size, temperature, combustion efficiency and composition of the products. Most of the experimental studies have been conducted to examine DC electric field effects on flames. At the atmospheric pressure and low DC electric field intensity ($E < 10^4$ V/cm) insufficient for the excitation and ionization of the flame compounds, the field-induced ionic wind effect on flame dominates, when the electric body force ($\mathbf{F} = \sum n_{i,e} e \mathbf{E}$) drives the positively charged flame species (CHO⁺, H₃O⁺, CH₃⁺ and C₃H₃⁺) in the field direction, resulting in a field-enhanced heat/mass transfer of neutral flame species with local variations of the flame composition and rate of reactions developing in the flame reaction zone [1–7]. In accordance with [8, 9], the DC electric field-enhanced processes of heat/mass transfer result in homogenization of the flame reaction zone, thus reducing the peak flame temperature and the rate of two-step reactions of NO_x formation by the Zeldovich mechanism, advancing a cleaner and more effective heat energy production.

Most of previous experimental studies were focused on the DC electric field effects on the flame behavior, when momentum transfer from the charged flame species to the neutrals results in field-induced ion wind effects determining variations of the bulk flow motion. By applying the AC electric field to the flame, the flame response to the applied electric field is affected both by variations of the AC field frequency (f) and by applied field voltage determining transition from ion wind effects to electro-chemical and thermal effects [10]. The average collision response time between the ions and neutral flame species that is required to generate the ion wind effect in the atmospheric pressure flame is about 10 ms [11]. This corresponds to the electric field frequency $f \approx 50$ Hz. Increasing the AC field frequency significantly reduces the time between oscillations by limiting the momentum transfer from the charged flame species to the neutrals and reduces the ion wind effect on the flame behavior [5, 9–11]. The results of the experimental investigation on the flame response to the AC field oscillations confirm [9–11] that the AC field effect on flame is a result of coupling between the ionic wind, electro-

chemical and thermal effects depending on the applied field frequency and voltage, which can lead to a distinctive flame behavior in low, mid-voltage and high-voltage regimes, when the electric-field-induced instability can occur and flames start oscillating [12–15]. Detailed understanding of the mechanism which is responsible for the field-induced flame oscillations is not clear, and a more detailed investigation into the processes of flame response to field-induced oscillations is still required. It should be noted that most experiments on AC electric field effects on flames can be related to laminar diffusion flames of gaseous fuels (methane), whereas studies on the effects of AC electric field on the flame formation at thermo-chemical conversion of biomass are highly limited [16, 17] and need to be deepened to get the insight into the effects of high-frequency oscillations on the thermal decomposition of biomass and on the combustion of volatiles. Therefore, this paper examines the flame behavior and the formation of the flame reaction zone at thermo-chemical conversion of wood pellets by comparing the field effects on the flame, when the flame base is subjected to a DC electric field and high-frequency AC oscillations.

1. Experimental setup. The experimental studies of DC and AC electric field effects on the processes of thermo-chemical conversion of biomass and heat energy production were carried out using a batch-size experimental setup of average heat power of 2–3 kW [18], as well as an experimental setup with continuous feeding of biomass (wood) pellets into the combustor with an average heat power up to 20 kW and a single electrode configuration, which is inserted through the biomass layer up to the flame reaction zone (Fig. 1).

The DC and AC electric fields of frequency 50 Hz and 13.56 MHz were applied in the space between the axially inserted electrode and the annular grounded electrode located at the bottom of the gasifier determining the formation of a current (I) across the high-resistance flame reaction zone ($R \approx M \Omega$) and low-resistance layer of wood pellets ($R \approx 1 - 10 \Omega$) that are subject to thermo-chemical conversion at biomass gasification and wood fuel carbonization. Note that the flame

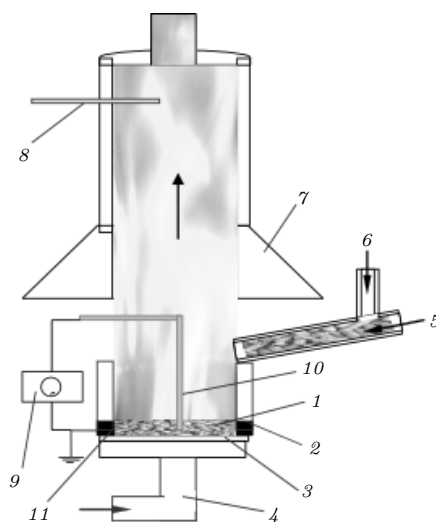


Fig. 1. Schematic of the experimental setup with continuous feeding of biomass pellets. 1 – gasifier with wood pellets; 2 – quartz channel; 3 – ceramic grate; 4 – primary hot air supply; 5 – feed of pellets; 6 – secondary hot air supply; 7 – combustor; 8 – diagnostic tools to measure flame temperature and composition; 9 – high-frequency generator; 10 – axially inserted electrode; 11 – annular grounded electrode.

conductivity increases just above the wood pellets, where the formation of primary charged flame species is observed decreasing the resistance below 10–100 k Ω . Provided the continuous feeding of wood pellets into the combustor (Fig. 1), an experimental study of the electric field effects on the combustion characteristics was carried out by varying the bias voltage of the axially inserted electrode, whereas the current I between the electrodes was limited to 20–25 A. The average power of high-frequency oscillations (13.56 MHz) was limited by the power of a high-frequency generator (600 W). In addition, experiments were carried out using the AC electric field of frequency 41 MHz that was applied across the flame base of the batch-size experimental setup [16].

The electric field effect on the main combustion characteristics was estimated providing the complex measurements of the flame temperature, composition, combustion efficiency and produced heat energy by varying the bias voltage of the axially inserted electrode relative to the grounded channel walls. Online measurements of the products temperature, composition and combustion efficiency were made using a Testo- 350XL gas analyzer and a sampling gas probe. Pt/Pt/Rh thermocouples were used for local online measurements of the flame temperature, whereas calorimetric measurements of cooling water flow were made to estimate the field effects on the heat energy production at thermo-chemical conversion of wood pellets [14].

2. Results and discussion. The modelling experiments on the flame response to the DC electric field using the batch-size pilot setup with a single electrode configuration have shown that the dominant feature of the electric field effect on the flame formation at thermo-chemical conversion of biomass pellets is the field-enhanced thermal decomposition of biomass pellets, which increases the average rate of the biomass weight loss (dm/dt) from 1 g/s for undisturbed flame ($I = 0$) to 1.5 g/s for the flame subject to the electric field, so increasing the average current between the electrodes up to 2 mA. The field-enhanced thermal decomposition of wood pellets results in an increase of the axial flow of volatiles (CO, H₂), their ignition and combustion with radial expansion of the flame reaction zone [16–18]. By increasing the DC voltage of the axially inserted electrode, the field-induced decrease of the peak flame temperature close to the flame axis (by 12%) was observed, which correlates with the field-enhanced increase of the produced heat energy by 12%. This correlation confirms the field-induced ion wind effect determining the enhanced heat/mass transfer of the flame species from the central reaction zone to the channel walls (Fig. 2).

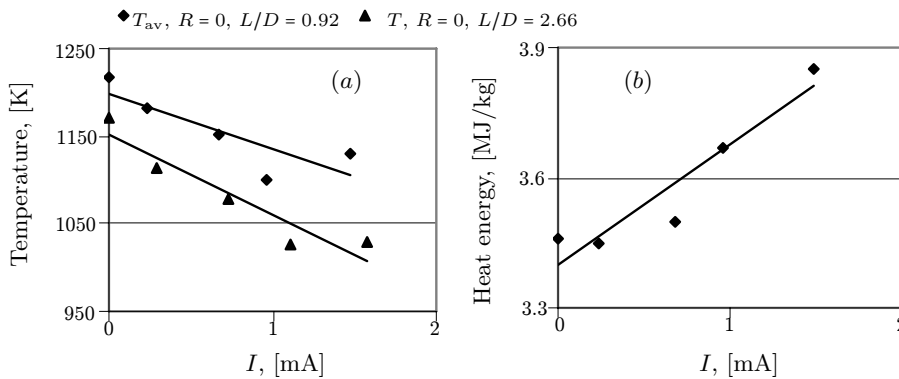


Fig. 2. DC electric field-induced variations of the flame temperature in the flame reaction zone (a) and the produced heat energy (b).

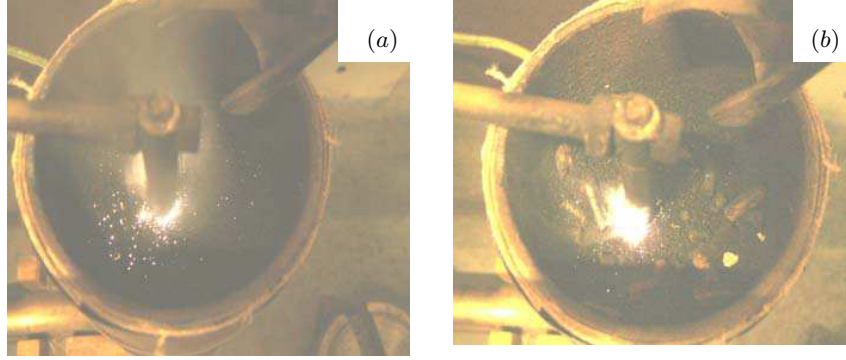


Fig. 3. The formation (a) and explosion (b) of hot spots on the surface of carbonized wood pellets by increasing the applied voltage and mean current across the wood layer.

If the electric field is applied at the bottom the combustor, with the heat power 20 kW and continuous feed of pellets, the main feature of the field-induced current in the space between the electrodes (Fig. 1) is the formation of discrete bright spots on the surface of wood pellets (Fig. 3a), indicating some analogy with the formation of surface plasmons [19]. This allows to suggest that by increasing of the applied voltage and applied field intensity (E) a mean value of the current density (1) in the space between the electrodes leads to local overheating of wood pellets promoting their thermal decomposition and carbonization with a correlating increase of the conductivity of carbonized wood pellets (2), whereas the resistance of the layer of carbonized pellets decreases to about 10Ω :

$$j = \frac{e^2 n_e}{\nu_e m_e} E, \quad (1)$$

$$\sigma = \frac{e^2 n_e}{\nu_e m_e} = \frac{\varepsilon_0 \omega_L^2}{\nu_e}, \quad (2)$$

$$\omega_L = e \sqrt{\frac{n_e}{\varepsilon_0 m_e}}, \quad (3)$$

where e is the electron charge, n_e and m_e are their density and mass, ν_e is the electron collision frequency with neutral species, E is the electric field intensity, ε_0 the dielectric constant, and ω_L is the Langmuir frequency.

The local overheating of carbonized pellets results in spots explosion that predominately is observed in the near vicinity of the central electrode indicating the formation of a corona discharge (Fig. 3b).

The corona discharge extends from the spots to the flame reaction zone and the flame becomes brighter with a correlating increase of the flame temperature depending on the applied field intensity ($T \approx E^2$), the degree of flame ionization n_e and the field-induced current density (j) across the flame reaction zone, whereas the current density across the layer of carbonized wood pellets decreases so limiting the local overheating of carbonized wood pellets and spots explosion. This, in turn, is a limiting step for the development of corona discharge and transition from undisturbed combustion conditions to plasma supported combustion producing instability, as it is observed if the electric field acts on the low-temperature plasma flow [15] and occurs under conditions when $T_e \sim E^2$ and $n_e \sim I$ (Fig. 4).

The impact of EM field on combustion

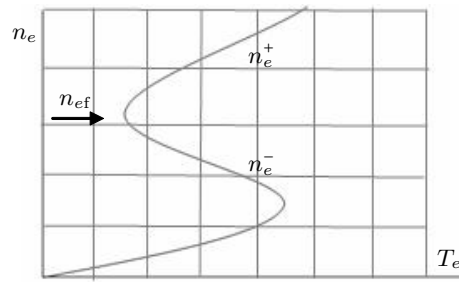


Fig. 4. S-type dependence of the electron density on the temperature T_e for the field-induced instability [15], where n_e^+ denotes equilibrium ionization conditions; n_e^- is non-equilibrium ionization; n_{eff} corresponds to $n_e^+ = n_e^- \approx 10^{11} \text{ cm}^{-3}$.

Visual observation of the hot spots formation reveals that the characteristic life-time of the hot spots formation is some seconds and their sizes are 1–10 mm. In order to estimate the effect of current distribution on the process stability, experiments with an external magnetic field (B_z) were performed. In the case when the magnetic field force $f_\varphi \sim j_r B_z$ is applied to the flame base and to the layer of carbonized pellets, the number of hot spots decreases with a correlating decrease of the mean value of the field-induced current, whereas the resistance of

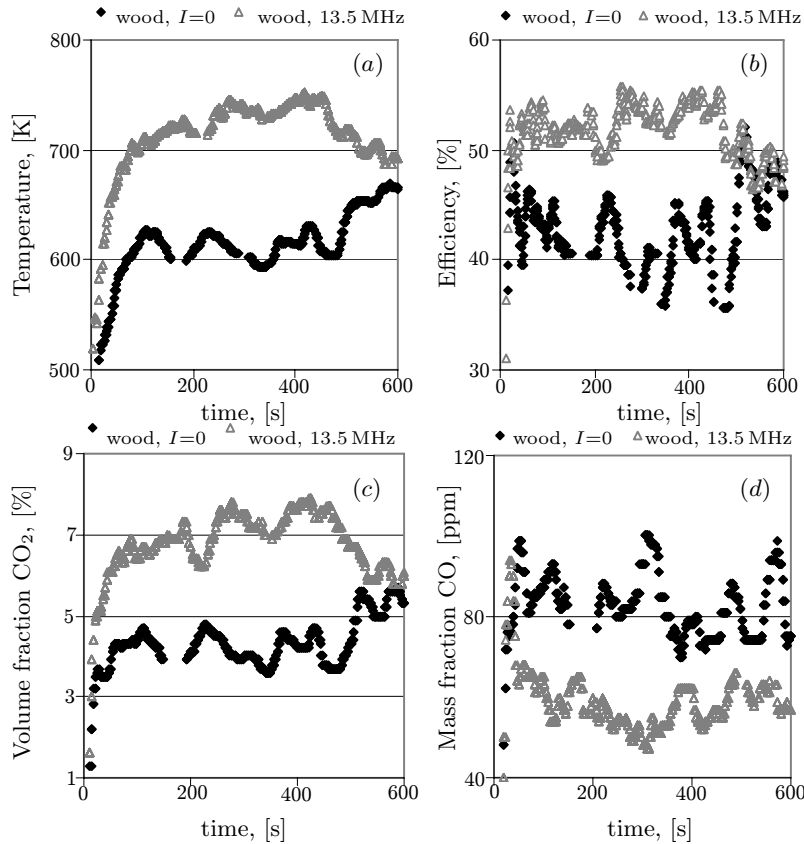


Fig. 5. AC electric field-induced variations of the flame temperature (a), combustion efficiency (b) and products composition (c), (d).

the carbonized wood layer increases. This allows to suggest that the magnetic field disturbs the current oscillations between the flame and carbonized wood pellets. Some experiments were performed under a radial magnetic field when $j \parallel B$. In that case, both the stability of the current distribution and the total current value increased.

Note that the non-stationary current distribution across the layer of carbonized pellets with the formation of discrete bright spots on the surface of the carbonized wood pellets was observed for all cases when the AC or the DC electric field was applied to the layer of carbonized wood pellets. By increasing the applied voltage, the spots start to explode initiating the formation of corona discharge in the vicinity of the axially inserted electrode with direct influence on the combustion characteristics developing at thermo-chemical conversion of wood pellets (Fig. 5). As follows from Fig. 5, the field-induced formation of corona discharge during spots explosion results in a rapid increase of the flame temperature by 21% and combustion efficiency by 13%, with the correlating increase of the volume fraction of the main product (CO_2) by 50%, whereas the air excess in the products decreases by 50% and the mass fraction of volatiles (CO) by 35%, evidencing that the plasma supported combustion results in a more effective thermo-chemical conversion of wood pellets.

When analyzing the field-enhanced thermal decomposition of carbonized wood pellets, it should be noted that there are some analogies with the known effects in conducting graphene when it attracts H or O to the free bonds, which leads to the formation of graphane with higher resistance [20–22]. In our case, the situation is quite opposite. At the starting point, the hydrocarbon bounds in hemicellulose,

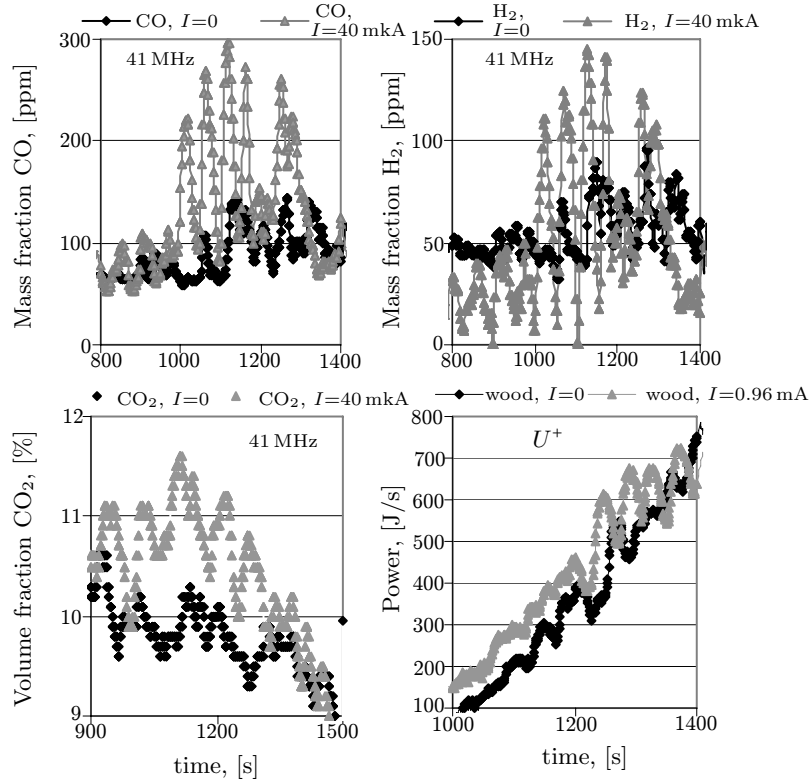


Fig. 6. AC ($f = 41$ MHz) and DC (U^+) electric field-induced oscillations of the flame composition and produced heat energy.

cellulose and lignin which are the main wood compounds, are saturated determining the formation of a high-resistive layer of wood pellets. During the thermal decomposition and carbonization of wood, hemicellulose, cellulose and lignin start decomposing and the resistance of the carbonized wood layer rapidly decreases with an inhomogeneous current distribution across the layer of carbonized wood pellets, which results in local overheating of the carbonized pellets and in formation of local hot spots with field-enhanced release of volatiles and field-enhanced transition to the regime of corona discharge at the spots explosion. The physical mechanism of the hot spots formation and their influence on the development of the combustion process is still unclear.

Finally, it should be stressed that in addition to the field-enhanced thermal decomposition of wood pellets and combustion of volatiles by the applied DC and AC electric fields to the flame base, the field-induced formation of corona discharge with the plasma supported combustion of volatiles results in the formation of field-induced instability [15], which leads to low-frequency (0.02 Hz) oscillations of the flame composition and produced heat energy at thermal decomposition of biomass in the gasifier (Fig. 6). In fact, the field-induced oscillations in the batch-size experimental setup predominately occurred during the after-flaming charge conversion stage in a time interval from $t = 800$ to 1400 s, when the thermal decomposition of hemicellulose, cellulose and lignin resulted in field-enhanced carbonization of wood pellets [23] with enhanced formation and explosion of spots that led to the transition of plasma supported combustion of volatiles (CO, H₂). The low frequency of the field-induced oscillations allows to suggest that the instability of the thermal decomposition at this stage of char conversion is a result of the instability of thermal processes developing during the formation of plasma supported combustion determining the field-enhanced oscillations of the current between the wood layer and the flame reaction zone.

3. Conclusion. The DC and AC electric field effects on the flame characteristics at thermo-chemical conversion of wood pellets for the configuration with a single electrode inserted through the wood layer of wood pellets up to the flame reaction zone have been studied and discussed.

The obtained results allow to conclude that for the given field configuration the field effect on the flame characteristics is initiated by the field-enhanced thermal decomposition and by the carbonization of wood pellets with field-enhanced ignition and combustion of volatiles. The increase in applied voltage results in the formation of hot spots in the carbonized wood layer and in spots explosion, determining the formation of corona discharge with the plasma supported combustion of the volatiles.

The formation of corona discharge leads to the formation of combustion instability with the development of low-frequency oscillations of the combustion characteristics at thermo-chemical conversion of the wood fuel. In fact, the main mechanism of the field-induced instability at thermo-chemical conversion of wood pellets is still unclear, and additional studies and process analysis are needed to determine the main factors that induce the observed low-frequency oscillations.

Acknowledgements. The authors would like to acknowledge the financial support of the ERAF project No. 2014/0051/2DP/2.1.1.1.0/14/APIA/VIAA/004

REFERENCES

- [1] J. LAWTON, F. WEINBERG. *Electric Aspects of Combustion* (Clarendon Press, Oxford, England, 1969), pp. 1–650.

- [2] H.C. JAGGERS, A. VON ENGEL. The effect of electric fields on the burning velocity of various flames. *Combustion and Flame*, vol. 16 (1971), pp. 275–285.
- [3] B.N. GANGULY. Hydrocarbon combustion enhancement by applied electric field and plasma kinetics. *Plasma Physics and Controlled Fusion*, vol. 49 (2007), pp. B239–B246.
- [4] D. DUNN-RUNKIN, F.J. WEINBERG. Using large electric fields to control transport in microgravity. *Annals of the New York Academy of Sciences*, vol. 1077 (2006), pp. 570–584.
- [5] M.K. KIM, S.K. RYU, S.H. WON, S.H. CHUNG. Electric fields effect on liftoff and blow off of nonpremixed laminar jet flames in a co flow. *Combustion and Flame*, vol. 157 (2010), pp. 17–24.
- [6] A.M. DREWS, L. CADEMARTIRU, M.L. CHEMAMA, M.P. BRENNER, G.M. WHITSIDES, K.J.M. BISHOP. AC electric fields drive steady flows in flames. *Physical Review*, vol. E86 (2012), pp. 036314–1–4.
- [7] A.YU. STARIKOWSKII. Plasma supported combustion. *Reports of the Combustion Institute*, vol. 30 (2005), pp. 2405–2417.
- [8] J. COLANNINI. *Electrodynamic Combustion Control™ Technology. A Clear Sign White Paper* (ClearSign Combustion Corporation, Seattle, 2012), www.clearsigncombustion.com.
- [9] C.H. BERMAN, R.J. GILL, H.F. CALCOTE. N_x reduction in flames stabilized by an electric field. Fossil Fuel Combustion. *ASME*, vol. 33 (1991), pp. 71–76.
- [10] Y. ZHANG, Y. WU, H. YANG, H. ZHANG, M. ZHU. Effect of high-frequency alternating electric fields on the behavior and nitric oxide emission of laminar non-premixed flames. *Fuel*, vol. 109 (2013), pp. 350–355.
- [11] M.K. KIM, S.H. CHUNG, H.H. KIM. Effect of AC electric fields on the stabilization of premixed Bunsen flames. *Reports of Combustion Institute*, vol. 33 (2011), N 11, pp. 1137–1144.
- [12] C.K. RYU, Y.K. KIM, M.K. KIM, S.H. WON, S.H. CHUNG. Observation of multi-scale oscillation of laminar lifted flames with low-frequency AC electric fields. *Combustion and Flame*, vol. 157 (2010), pp. 25–32.
- [13] M. BELHI, P. DOMINGO, P. VERVISH. Effect of electric field on flame stability. *Proc. the European Combustion Meeting* (2009), pp. 1–6.
- [14] R. ANBARAFSHAN, H. AZIZINAGSH, R.M. NAMIN. Flames in horizontal electric field, deviation and oscillation. *Proc. IYPT* (2012), pp. 1–8, http://archive.iypt.org/iypt_book/2011.3_Bouncing_flame_Iran_RM_NHARA_v3.pdf.
- [15] L.M. BIBERMAN *et al.* *Kinetics of Nonequilibrium Low-Temperature Plasmas* (Paperback, 2012), pp. 1–498.
- [16] I. BARMINA, A. ČIPIJS, A. LĪCKRASTIŅA, J. VALDMANIS, R. VALDMANIS, M. PURMALIS, M. ZAĶE. Renewable fuel gasification and combustion control by applied AC electric field. *Proc. the 8th International Pamir Conference on Fundamental and Applied MHD* (France, 2011), vol. 2, pp. 843–847.

- [17] I. BARMINA, M. PURMALIS, R. VALDMANIS, J. VALDMANIS, M. ZAĶE. Active control of the biomass combustion characteristics with high frequency oscillations. *Proc. the 12th International Conference "Engineering for Rural Development* (Jelgava, Latvia, 2013), no. 120, pp. 648–652.
- [18] I. BARMINA, R. VALDMANIS, M. ZAĶE. The electric field effect on combustion dynamics. *Proc. the 9th International Pamir Conference on Fundamental and Applied MHD. Thermo Acoustic and Space Technologies* (Riga, Latvia, 2014), vol. 1, pp. 33–37.
- [19] M.J. STOKMAN. Nanoplasmonics: The physics behind the applications. *Physics Today*, vol. (2011), pp. 39–44.
- [20] M. KAURANEN, A.V. ZAYATS. Nonlinear plasmonics. *Nature Photonics*, vol. 6 (2012), pp. 737–748.
- [21] S.F. SHI *et al.* Controlling graphene ultrafast hot carrier response from metal-like to semiconductor-like by electrostatic gating. *Nano Lett.*, vol. 14 (3) (2014), pp. 1578–1582.
- [22] Z.K. LIU *et al.* Discovery of a three-dimensional topological Dirac-semimetal. *Science*, vol. (2014), pp. 864–867.
- [23] I. BARMINA, A. LĪCKRASTIŅA, J. VALDMANIS, R. VALDMANIS, M. ZAĶE, A. ARSHANITSA, G. TELYSHEVA, V. SOLODOVNIK. Effect of microwave pre-processing of pelletized biomass on gasification and combustion characteristics. *Latvian Journal of Physics and Technical Sciences*, vol. 4 (2013), pp. 34–48.

Received 14.01.2015